Published in final edited form as:
Biochemistry. 2008 August 12; 47(32): 8358–8366. doi:10.1021/bi800631h.

Allosteric Coupling in Pyruvate Dehydrogenase Kinase 2†

Alla Klyuyeva, **Alina Tuganova**, and **Kirill M. Popov***
Department of Biochemistry and Molecular Genetics, Schools of Medicine and Dentistry, University of Alabama at Birmingham, Birmingham, Alabama 35294 *Received April 9, 2008; Revised Manuscript Received June 4, 2008*

Abstract

Mitochondrial pyruvate dehydrogenase kinase 2 (PDHK2) phosphorylates the pyruvate dehydrogenase multienzyme complex (PDC) and thereby controls the rate of oxidative decarboxylation of pyruvate. The activity of PDHK2 is regulated by a variety of metabolites such as pyruvate, NAD^+, NADH, CoA, and acetyl-CoA. The inhibitory effect of pyruvate occurs through the unique binding site, which is specific for pyruvate and its synthetic analogue dichloroacetate (DCA). The effects of NAD^+, NADH, CoA, and acetyl-CoA are mediated by the binding site that recognizes the inner lipoyl-bearing domain (L2) of the dihydrolipoyl transacetylase (E2). Both allosteric sites are separated from the active site of PDHK2 by more than 20 Å. Here we show that mutations of three amino acid residues located in the vicinity of the active site of PDHK2 (R250, T302, and Y320) make the kinase resistant to the inhibitory effect of DCA, thereby uncoupling the active site from the allosteric site. In addition, we provide evidence that substitutions of R250 and T302 can partially or completely uncouple the L2-binding site. Based on the available structural data, R250, T302, and Y320 stabilize the "open" and "closed" conformations of the built-in lid that controls the access of a nucleotide into the nucleotide-binding cavity. This strongly suggests that the mobility of ATP lid is central to the allosteric regulation of PDHK2 activity serving as a conformational switch required for communication between the active site and allosteric sites in the kinase molecule.

Pyruvate dehydrogenase kinase (PDHK)[1] phosphorylates the mitochondrial pyruvate dehydrogenase multienzyme complex (PDC) and thereby downregulates the rate of aerobic oxidation of carbohydrate fuels (1,2). In mammals, there are at least four genetically and biochemically distinct forms of PDHK (PDHK1, PDHK2, PDHK3, and PDHK4) (3,4). Growing evidence strongly suggests that PDHK isozymes play specialized roles in regulation of PDC (1,2). Two isozymes are implicated in the long-term control of PDC under conditions of oxygen (5) or food (6) deprivation (PDHK1 and PDHK4, respectively). The isozyme PDHK2 is primarily involved in the short-term control of PDC mediating the effects of different metabolites such as pyruvate, NAD^+, NADH, CoA, and acetyl-CoA (7). The physiological role of PDHK3 in the regulation of PDC activity remains largely unknown.

It is generally believed that PDHK2 operates as an integral component of PDC attached to the inner lipoyl-bearing domain (L2) of dihydrolipoyl transacetylase (E2) (8,9). Binding to E2 greatly increases the ability of PDHK2 to phosphorylate multiple copies of pyruvate

†This work was supported by Grant GM51262 from the U.S. Public Health Service.

*Address correspondence to this author. Telephone: (205) 996-4065. Fax: (205) 934-0758. E-mail: kpopov@uab.edu.

[1]Abbreviations: PDC, pyruvate dehydrogenase complex; PDHK, pyruvate dehydrogenase kinase; PDHK1, PDHK2, PDHK3, and PDHK4, isozymes 1, 2, 3, and 4 of pyruvate dehydrogenase kinase; E1, pyruvate dehydrogenase component of PDC; E2, dihydrolipoyl transacetylase component of PDC; E3, dihydrolipoyl dehydrogenase component of PDC; E3BP, E3-binding protein component of PDC; L2, the inner lipoyl-bearing domain of dihydrolipoyl transacetylase; DCA, dichloroacetate; Lyp, lipoic acid; SDS/PAGE, polyacrylamide gel electrophoresis in the presence of sodium dodecyl sulfate; DTT, dithiothreitol; ITC, isothermal titration calorimetry; DMSO, dimethyl sulfoxide.

dehydrogenase (E1) attached to the E2 scaffold (8). At the same time, association with E2 allows for the regulation of PDHK2 activity by NAD^+, NADH, CoA, and acetyl-CoA (10). These metabolites affect PDHK2 activity indirectly by changing the oxidation and acetylation states of the lipoate prosthetic groups of L2 domains (11). Kinase activity is the lowest when lipoate groups are fully oxidized (11). Their NADH-dependent reduction catalyzed by dihydrolipoyl dehydrognase (E3) causes a significant increase in the rate of phosphorylation. This rate can be increased even further when the reduced lipoates are acetylated by E2 using acetyl-CoA as a substrate (11). All of these effects are L2 mediated and, consequently, require an association of kinase with E2. In contrast, the effect of pyruvate on PDHK2 activity can be observed in the absence of E1 and E2, suggesting that pyruvate inhibits kinase activity directly (1,2).

The complexity of allosteric control of PDHK2 activity prompted a number of studies aimed at its structural characterization (12,13). These studies revealed that PDHK2 consist of two domains: the amino-terminal domain (R domain) assembled as a four-helix bundle and the carboxy-terminal domain (K domain) folded as a mixed α/β sandwich (12). K domain carries the nucleotide-binding site, while the E1-binding site is likely to be located on the interface between K and R domains (12). The binding site for synthetic analogue of pyruvate, dichloroacetate (DCA), has been identified in the middle of R domain (13). It is separated from the active site by more than 20 Å. The lipoate-binding site is located on the tip of R domain and is more than 30 Å away from the active site (14).

Evidence presented by this and other laboratories suggests that adenine nucleotides play an intimate role in the regulation of PDHK2 activity (15–17). For example, it has been demonstrated that binding of ADP significantly increases binding of DCA, while binding of DCA aids in binding of ADP (15). In addition, a cross-talk has been observed betweentheL2-andnucleotide-binding sites of PDHK2 (15,17). Adenine nucleotides have been shown to decrease the affinity of PDHK2 for the L2 domain (15). Conversely, L2 binding decreases PDHK2 affinity for adenine nucleotides (15,17). These observations prompted Bao and colleagues to propose that the strength of ADP binding is central to the allosteric control of PDHK2 activity (11,18). According to the authors, allosteric inhibitors, such as pyruvate and DCA, act by decreasing the rate of dissociation of ADP (18). On the other hand, allosteric activators stimulate PDHK2 activity by increasing the rate of ADP dissociation (11). Thus, the adenine nucleotides indisputably play an important role in the regulation of PDHK2 activity. However, the molecular mechanisms responsible for the allosteric coupling between the active site and allosteric sites in PDHK2 molecule remain enigmatic. This study was undertaken in order to identify the structural elements of PDHK2 molecule that are essential for the long-distance communications between the nucleotide-binding and allosteric sites of PDHK2. Here, we present evidence that the ATP lid, which is a flexible loop that encloses the nucleotide in its binding cavity, plays a key role in the allosteric coupling.

EXPERIMENTAL PROCEDURES

Vector Construction and Protein Expression

Bacterial expression vectors for E1, E2/E3BP subcomplex, lipoyl-protein ligase A, GST-L2 (amino acids Ser 127 to Ile 214), His_6-L2 (amino acids Ser 127 to Ile 214), and PDHK2 were constructed as described previously (7,19–21). Mutations in the sequence of rat PDHK2 cDNA (22) were introduced by site-directed mutagenesis (23) using pPDHK2 expression vector (7) and following oligonucleotide primers: GCG GCC ACA GTG GAA AGC CA for R250 to A mutation, GCA GCT CCT ACA CCC CAG CC for T302 to A mutation, and CC CGC CTC TTC GCC AAG TAC TTC CA for Y320 to F mutation; altered bases are underlined. Reactions were carried out using the ExSite site-directed mutagenesis kit (Stratagene, La Jolla, CA) essentially as recommended by the manufacturer. Mutations and fidelity of PDHK2 cDNA

were verified by sequencing (24). E1, E2/E3BP subcomplex, GST-L2, His_6-L2, wild-type PDHK2, and its mutants were expressed and purified following the established protocols (7, 19–21). The protein composition of each protein preparation was evaluated by SDS/PAGE analysis. Gels were stained with Coomassie R250. All preparations used in the present study were more than 90% pure.

Kinase Activity Assay

PDHK2 activity was measured at 37 °C as the rate of [^{32}P]phosphate incorporation into the E1 protein using [γ-^{32}P]ATP (7). A typical reaction mixture (50 μL) contained 26 μg of E1, 24 μg of E2/E3BP, 0.5 μg of PDHK2, and 0.5 mM [γ-^{32}P]ATP (specific activity of 100–200 cpm/pmol) in 20 mM Tris-HCl (pH 7.8), 5 mM $MgCl_2$, 50 mM KCl, 5 mM DTT, and 2.0% (v/v) ethylene glycol. The phosphorylation mixtures were preheated at 37 °C for 60 s. The reactions were initiated by the addition of 5 μL of ATP solution and terminated after 60 s incubation by spotting 40 μL of the reaction mixture onto 2.1 cm diameter disk of Whatman 3MM paper presoaked in a solution of 20% (w/v) trichloroacetic acid, 0.2 M phosphoric acid, 50 mM sodium pyrophosphate, and 50 mM ATP. After extensive washing with 10% (w/v) trichloroacetic acid, the protein-bound radioactivity was determined by liquid scintillation counting. A negative control (minus PDHK2) was used to determine the nonspecific incorporation. All assays were conducted in triplicates.

GST-L2 Pull-Down

The interaction of PDHK2 with GST-L2 was studied using pull-down assay as described previously (25). Briefly, binding experiments were performed at room temperature in Spin-X microcentrifuge filter device with a pore diameter of 0.22 μm (Corning Inc., Corning, NY). A typical binding mixture (400 μL) contained 40 μg of PDHK2 and 25 μL (v/v) of settled glutathione-Sepharose beads decorated with 100 μg of GST-L2 in 25 mM Tris-HCl buffer (pH 8.0), 0.1 mM EDTA, 2.5 mM $MgCl_2$, 0.1 M KCl, 5 mM dithiothreitol, 1% (v/v) glycerol, and 0.1 mg/mL BSA. When required, ATP, ADP, DCA, or a combination of DCA and ATP or ADP was included at the indicated concentrations. For experiments employing high concentration of ATP or ADP, the binding buffer was supplemented with 13 mM $MgCl_2$. The reaction was initiated by the addition of 40 μg of PDHK2. After incubation for 10 min, unbound PDHK2 was removed by centrifugation for 1 min at 6000*g* followed by three consecutive washes in 0.4 mL of binding buffer. Bound PDHK2-GST-L2 complexes were eluted in 0.1 mL of binding buffer supplemented with 10 mM reduced glutathione. Free and bound PDHK2 were analyzed using SDS/PAGE. Gels were stained with Coo-massie R250. Stained gels were analyzed by scanning densitometry using UN-SCAN-IT automated digitizing system (Silk Scientific, Inc., Orem, UT).

ATP, ADP, and DCA Binding

Binding of ATP, ADP, or DCA to PDHK2 was measured at 25 °C following the quenching of PDHK2 intrinsic tryptophan fluorescence as described by Hiromasa and colleagues (15). Binding reaction of the initial volume of 2.0 mL containing 1 μM PDHK2 in 50 mM potassium phosphate buffer (pH 7.5), 0.5 mM EDTA, and 2.0 mM $MgCl_2$ was carried out in standard (1 × 1 cm) cuvettes. When required, ADP or DCA was included at the indicated concentration. The appropriate ligands, i.e., ATP, ADP, or DCA, were added in 2–5 μL increments with constant stirring. Steady-state fluorescence of PDHK2 was recorded using Cary Eclipse fluorescence spectrophotometer (Varian Inc., Palo Alto, CA). Sample was excited at 290 nm (slit 5 nm), and emission was recorded at 350 nm (slit 5 nm). Titrations with AMP or acetic acid were performed as controls and were used to correct the experimental data. Background-corrected results were analyzed essentially as described by Hiromasa et al. (15). The

concentrations of ATP, ADP, and AMP were evaluated based on their absorbance coefficient $\varepsilon = 1.54 \times 10^4\ M^{-1}\ cm^{-1}$ at 259 nm.

Isothermal Titration Calorimetry (ITC)

The interaction of PDHK2 with L2 was characterized by ITC (25). L2-binding measurements were carried out at 30 °C in 20 mM potassium phosphate buffer (pH 7.5), 50 mM KCl, 10 mM $MgCl_2$, 5 mM dithiothreitol, and 2% (v/v) ethylene glycol. The concentration of PDHK2 in the calorimeter cell was 20 μM. The concentration of L2 in the injection syringe was 520 μM. Injections were made in 10 μL increments with 240 s spacing between the injections. For L2-binding experiments in the presence of ATP, ATP was added to both the cell and syringe to the final concentration of 10 mM. The concentration of $MgCl_2$ in these experiments was increased to 13 mM. Dissociation constants (K_d) and enthalpy changes (ΔH) were obtained using the Origin software package (version 7.0) provided by the manufacturer (OriginLab, Northampton, MA).

Statistical Analysis

The reported parameters represent the means ± standard deviation obtained for at least three independent determinations. Statistical analysis was performed by an unpaired Student's *t*-test. $P < 0.05$ was considered to be statistically significant.

Other Assays

SDS/PAGE was carried out according to Laemmli (26). Protein concentrations were determined according to Lowry (27) with bovine serum albumin as a standard. The extent of L2 lipoylation was examined following the procedure described by Quinn and colleagues (28); the lipoate content of all L2 constructs was greater than 90%.

RESULTS AND DISCUSSION

Conformation of ATP Lid in PDHK2

Examination of several PDHK2 structures available through the RCSB Protein Data Bank (PDB accession numbers 1jm6, 2bu2, and 2bu8) shows that ATP lid is the only structural element in PDHK2 that displays significant rearrangement upon the nucleotide binding. The greatest differences are observed in the proximal part of ATP lid that assumes either "open" or "closed" conformation (Figure 1A). In its "open" conformation, the entire segment of ATP lid corresponding to the amino acids 296–302 (coordinate file 2bu2) is more than 10 Å apart from the nucleotide-binding cavity and is engaged in extensive interactions with the R domain. In "closed" conformation, this part of ATP lid (amino acids 296–304) extends over the bound nucleotide, thereby enclosing it inside the nucleotide-binding cavity (Figure 1A).

Quite remarkably, one amino acid residue of ATP lid, i.e., T302, appears to be involved in stabilization of both the "open" and the "closed" conformations. In "closed" conformation, it can form a number of hydrogen bonds with 2′-and 3′-hydroxyls of the bound nucleotide, as well as with R250 that extends from the opposite side of the nucleotide-binding cavity (Figure 1B). R250, in turn, can also engage the 3′-hydroxyl group of nucleotide, thus completing a highly interlocked hydrogen-bonding network that keeps the ATP lid attached to the nucleotide and to the rest of the nucleotide-binding cavity. As illustrated in Figure 1C, T302 stabilizes the "open" conformation through the hydrogen bonding to Y320.

Considering that ATP lid is the only structural element that significantly varies in conformation as a result of nucleotide binding, it is feasible that ATP lid movement triggers a sequence of signaling events that affect the allosteric sites in PDHK2 molecule. To test this hypothesis, we

created PDHK2 mutants carrying substitutions of T302, R250, and Y320 and characterized their enzymatic activities and regulation.

ATP, DCA, and L2 Binding by PDHK2 Mutants

In order to disrupt the hydrogen-bonding networks stabilizing ATP lid of PDHK2 in "open" and "closed" conformations, we used site-directed mutagenesis to substitute Y320 for F, T320 for A, and R250 for A. Based on structural considerations, the substitution of Y320 for F removes the hydrogen bond that stabilizes the "open" conformation. The substitution of R250 for A removes the hydrogen bond between R250 and T302 that forms when ATP lid is "closed". Finally, mutation of T302 to A affects both "open" and "closed" conformations. The resulting mutant PDHK2 proteins were expressed in bacteria along with wild-type PDHK2 and purified essentially as described previously (7).

Highly purified PDHK2 mutants were characterized for their ability to bind adenine nucleotides, DCA, and L2 domain (Table 1 and Figure 2). In agreement with the structural data showing that Y320 does not contribute to nucleotide binding, the substitution of Y320 for F had little, if any, effect on the binding of either ATP or ADP (K_d of 2.5 μM versus 1.7 μM and 10.6 μM versus 8.9 μM for ATP and ADP, respectively). In contrast, the mutation of T302 or R250 had a marked effect on the affinity of PDHK2 for adenine nucleotides. As illustrated in Figure 2A, the affinities of PDHK2-T302A and PDHK2-R250A for ATP decreased more than 20-fold and 30-fold, respectively, relative to that of wild-type PDHK2. Similar or even greater effects were exerted by these mutations on PDHK2 affinity for ADP. However, the inner filter effect precluded accurate determination of ADP-binding constants for either PDHK2-T302A or PDHK2-R250A.

As discussed under the introduction, the DCA- and L2-binding sites of PDHK2 are located on R domain and are separated from the nucleotide-binding site, which is located on K domain, by 20 and 30 Å, respectively (13,14). In PDHK2 structure, neither of these sites is positioned in the vicinity of R250, T302, or Y320. In accord with the structural data, we found that mutant PDHK2 proteins bind DCA and L2 domain similarly to wild-type PDHK2 (Table 1 and Figure 2B), suggesting that both sites are properly folded and functional.

Thus, as it would be expected based on structural considerations, the substitution of Y320 had no appreciable effect on the binding of adenine nucleotides, DCA, or L2 by mutant PDHK2, while the mutation of R250 or T302 residues did not affect the DCA- and L2-binding sites of the kinase. At the same time, mutations of R250 and T302 exerted significant effect on PDHK2 affinity for adenine nucleotides, which is consistent with the structural data showing that R250 and T302 interact with the hydroxyl groups of ribosyl moiety of the bound nucleotide.

Enzymatic Activities of PDHK2 Mutants

To evaluate the functional consequences of substitution of R250, T302, and Y320 residues, the corresponding kinases were examined using standard phosphorylation assay. As shown in Figure 3A, the activity of PDHK2-Y320F was slightly lower than that of wild-type PDHK2. The activity of PDHK2-R250A was about 30% of the wild-type kinase, whereas the activity of PDHK2-T302A was significantly lower (approximately 10% of that of wild-type kinase).

Normally, the complex-bound PDHK2 readily phosphorylates 25–30 copies of E1 attached to E2 scaffold to the stoichiometry of 1.2 to 1.6 mol of phosphate incorporated/mol of E1 (19, 29). Under the current assay conditions, wild-type PDHK2 phosphorylated E1 to the stoichiometry of 1.3:1, while PDHK2-R250A phosphorylated E1 to the stoichiometry of 1.1:1 (Figure 3B). In contrast, the stoichiometry of E1 phosphorylation by PDHK2-T302A was just

0.4:1. It did not exceed that of 0.5:1 even when phosphorylation reaction was allowed to proceed for more that 60 min (Figure 3B).

Taken together, these data suggest that PDHK2-T302A and to a lesser extent PDHK2-R250A are defective in their ability to phosphorylate PDC. This defect does not stem from the lower affinity for nucleotide substrate displayed by these kinases. The low phosphorylation stoichiometry observed for PDHK2-T302A suggests that this kinase cannot phosphorylate all copies of E1 attached to the E2 scaffold, indicating that PDHK2-T302A encounters problems in accessing multiple copies of the protein substrate.

Communication between the Nucleotide- and DCA-Binding Sites in PDHK2 Mutants

Recently, Hiromasa and colleagues (15) have established that communication between the DCA-and nucleotide-binding sites of PDHK2 causes a significant increase in kinase affinity for one ligand when measurements are conducted in the presence of another ligand, i.e., ADP increases PDHK2 affinity for DCA, while DCA increases PDHK2 affinity for ADP. In this study, we used an assay based on the internal fluorescence quenching (15) in order to assess the effect of PDHK2 mutations on the cross-talk between DCA- and nucleotide-binding sites in kinase molecule. As illustrated in Figure 4A, under the conditions employed here, ADP caused a 19-fold increase in the affinity of wild-type PDHK2 for DCA. The affinity of wild-type PDHK2 for ADP was approximately 5 times greater in the presence of DCA (Figure 4B). The substitution of Y320 for F was associated with a small, but significant decrease in the effectiveness of the cross-talk between DCA- and nucleotide-binding sites (Table 2). The affinity of PDHK2-Y320F for DCA was just 9-fold greater in the presence of ADP, while DCA increased the affinity for ADP by a factor of 3.5. Importantly, far greater effects were observed for PDHK2-R250A and PDHK2-T302A mutants (Table 2). Under the standard conditions, i.e., in the presence of 50 μM ADP, the affinity of PDHK2-R250A for DCA increased only 2-fold, while the affinity of PDHK2-T302A for DCA was just 1.3-fold greater. Measurements conducted using greatly elevated concentrations of ADP (500 μM) gave a 5-and 3-fold increase in the affinity for DCA for PDHK2-R250A and PDHK2-T302A, respectively. Finally, both mutant kinases showed some DCA-induced increase in ADP binding (data not shown). However, due to inherently low affinity for ADP displayed by these kinases, it was difficult to evaluate this effect quantitatively.

DCA was shown to be a nonlinear, partial inhibitor of PDHK2 activity (18). Here, the effect of DCA on the activity of wild-type PDHK2 and its mutants was characterized in the standard phosphorylation assay. As illustrated in Figure 5, DCA effectively inhibited the activity of wild-type PDHK2. This effect developed in a concentration-dependent manner with the IC_{50} of approximately 0.69 mM. Control experiments carried over a wide range of sodium acetate concentrations revealed a slight decrease in PDHK2 activity that exhibited a linear relationship with the concentration of sodium acetate used in the assay. Quite remarkably, when similar experiments were conducted with PDHK2-R250A, PDHK2-T302A, and PDHK2-Y320F, neither of the mutant kinases displayed an effect of DCA that would significantly exceed that of sodium acetate (Figure 5).

Thus, all PDHK2 mutants examined here demonstrated a deficiency in communication between the DCA- and nucleotide-binding sites, indicating that ATP lid is important for the allosteric coupling. Judging from the DCA- and ADP-binding experiments, the severity of the defect appeared to be the greatest for PDHK2-R250A and PDHK2-T302A. These mutant kinases also had a reduced affinity for ADP. This brings about a possibility that the lack of the effect of DCA on the activity of these mutant kinases stems exclusively from the weak ADP binding. However, this explanation contradicts our observations on PDHK2-Y320F protein. In ADP-binding assay this kinase behaved similarly to the wild-type enzyme (K_d 8.9 μM versus 10.6 μM for PDHK2-Y320F and wild-type PDHK2, respectively). Its affinity for ADP

determined in the presence of DCA was also comparable to that of the wild type (2.5 μM versus 2.0 μM). However, DCA did not display an appreciable inhibitory effect on the activity of PDHK2-Y320F. Together, these observations strongly suggest that the increase in the strength of ADP binding is insufficient for the allosteric inhibition of PDHK2 activity by DCA.

Communication between the Nucleotide- and L2-Binding Sites in PDHK2 Mutants

Previously, we demonstrated that the amount of PDHK2 that could be recovered in the GST-L2 bound form was greatly decreased when pull-down experiments were conducted in the presence of ATP or ADP, suggesting that adenine nucleotides can regulate the interaction between PDHK2 and L2 (16). Here, we used this assay to screen PDHK2 mutants for their ability to bind L2 in a nucleotide-dependent manner. Initial experiments were conducted under the conditions that were established in the earlier study (16) that employed ATP and ADP at the final concentration of 0.5 mM each. As shown in Figure 6A, under these conditions, PDHK2-Y320F behaved similarly to the wild-type kinase; i.e., both ATP and ADP caused a significant decrease in the amount of PDHK2-Y320F bound to L2 with ATP being somewhat more potent than ADP. DCA added alone had little, if any, influence on L2 binding. However, when used in combination with ATP or ADP, DCA potentiated the effects of adenine nucleotides, which was especially apparent for DCA and ADP mixtures. In marked contrast, under these conditions adenine nucleotides had no appreciable effect on L2 binding to either PDHK2-R250A or PDHK2-T302A (Figure 6A). The failure of ATP and ADP to control L2 binding by PDHK2-R250A and PDHK2-T302A could be due in part to insufficient concentration of nucleotides in the assay mixture, because these kinases displayed a significantly reduced affinity for adenine nucleotides. To investigate this possibility, we conducted pull-down experiments using a high concentration of adenine nucleotides (10 mM each). As a control for nonspecific effects of ATP and ADP, we employed PDHK2-N247Q that cannot bind nucleotides (30). As illustrated in Figure 6B, PDHK2-N247Q did not display any nucleotide-dependent L2 binding, indicating that the elevated concentration of either ATP or ADP did not exert any nonspecific effects. Importantly, under these conditions, PDHK2-T302A also did not exhibit any appreciable effect of adenine nucleotides on L2 binding, suggesting that the nucleotide- and L2-binding sites in PDHK2-T302A were uncoupled (Figure 6B). In contrast, PDHK2-R250A demonstrated some nucleotide-dependent L2 binding, indicating, that, at least in part, the low affinity for adenine nucleotides accounts for the poor communication between the nucleotide- and L2-binding sites in PDHK2-R250A. However, the effects of adenine nucleotides on PDHK2-R250A were significantly weaker than on wild-type PDHK2, suggesting that the mutation of R250 partially uncouples the nucleotide- and L2-binding sites as well.

Recently, isothermal titration calorimetry (ITC) was successfully used to characterize the interactions between PDHK isozymes and L2 (17,25). In this study, we employed ITC to quantify the interactions between PDHK2-T302A and L2. Titration experiments in which L2 domain in the syringe was titrated into the reaction cell containing wild-type PDHK2 or PDHK2-T302A protein gave characteristic exothermic interactions (Figure 7A). For wild-type PDHK2, the fit of L2-binding data yielded dissociation constant (K_d) of 9.7 μM and enthalpy change (ΔH) of −14.5 kcal·mol^{-1}, which is in a good agreement with the results published earlier (25). Binding of L2 to PDHK2-T302A protein gave a somewhat greater enthalpy change of −21.7 kcal·mol^{-1} and dissociation constant of 6.3 μM. To examine the effect of adenine nucleotides on L2 binding, we performed experiments in which both cell and syringe solutions contained 10 mM ATP (Figure 7B). Under these conditions, a very small amount of molecular heat was released when wild-type PDHK2 was titrated with L2 domain, which is indicative of a weak binding. In contrast, titration of PDHK2-T302A with L2 domain generated good binding isotherms (Figure 7B). On average, this binding event was characterized by the

dissociation constant of 6.5 μM and enthalpy change of −16.6 kcal·mol^{-1}, indicating that ATP has little, if any, effect on L2 binding by PDHK2-T302A.

Thus, PDHK2-T302A did not display an appreciable effect of adenine nucleotides on L2 binding. This indicates that substitution of T302 for A can uncouple the nucleotide- and L2-binding sites in PDHK2 molecule, thereby providing evidence that the conformation of ATP lid is essential for the cross-talk between these sites.

CONCLUDING REMARKS

In this study, we created single amino acid substitutions that destabilize the "open" and "closed" conformations of ATP lid in PDHK2 (PDHK2- R250A, PDHK2-T302A, and PDHK2-Y320F). Biochemical analysis of the respective mutant kinases strongly suggests that ATP lid indeed plays a critical role in allosteric control of PDHK2 activity, which is evidenced by the data showing that all three mutations disrupt the allosteric regulation of PDHK2 by DCA, while two mutations (R250 to A and T302 to A) partially or completely uncouple the nucleotide- and L2-binding sites.

Previously, the allosteric regulation of kinase activity was rationalized in terms of control over the rate of dissociation of ADP (11,18). According to this hypothesis, allosteric inhibitors, such as DCA, inhibit kinase activity by reducing the rate of dissociation of ADP (18), whereas the allosteric activators, such as reduced and acetylated L2 domain, stimulate kinase activity by promoting dissociation of ADP (11). However, the behavior of PDHK2-Y320F contradicts this hypothesis. This enzyme binds ADP and DCA similarly to the wild-type kinase. DCA causes a significant increase in its affinity for ADP. Nevertheless, DCA has no appreciable effect on PDHK2-Y320F kinase activity. These observations strongly suggest that other mechanisms besides the control over the strength of ADP binding play a role in the regulation of kinase activity.

Some of these mechanisms can be inferred from the available structural data (12,13). The majority of PDHK2 structures containing bound nucleotides were obtained by soaking crystals of apo-PDHK2 in its "active" conformation (13). Consequently, they do not show any significant conformational changes caused by nucleotide binding. However, in one of the earlier studies the crystals of PDHK2-ADP complex were made *de novo* by cocrystallization of PDHK2 with an inhibitor (12). Thus, it is likely that this structure shows an "inactive" conformation of PDHK2. Comparison of the "active" and "inactive" conformations of PDHK2 reveals significant differences (Figure 8A). The "inactive" conformation of PDHK2 shows an interdomain hinge movement that closes up the cleft between K and R domains and causes a significant rearrangement in the structure of the active site. In the "active" conformation of PDHK2, Y320 is engaged with T302 when ATP lid is "open" (Figure 8B, left panel). To date, there is no structure of "active" PDHK2-ATP complex with ATP lid closed. However, Kato and colleagues (14) reported the structure of related PDHK3 isozyme in its "active" conformation with ATP lid closed. As illustrated in Figure 8B, middle panel, lid closing breaks bonding between T307 and Y326 (T302 and Y320 in PDHK2) and allows Y326 to engage Y155 (Y151 in PDHK2). In marked contrast, in the "inactive" conformation of PDHK2-ADP complex, Y320 shifts away from Y151 as a result of interdomain hinge movement. This disrupts the existing bonding network and allows Y320 to turn by almost 90° and occupy the access channel for protein substrate that under normal circumstances leads to the γ-phosphate of bound ATP (Figure 8B, right panel). This creates a conformation that is deficient with respect to its ability to support phosphorylation reaction. Taken together, these structural and biochemical data indicate the existence of highly integrated regulatory mechanism whereby the ADP-induced movement of ATP lid accompanied by the inter-domain hinge movement is

coupled with the rotation of Y320 that allows Y320 to block the access channel for protein substrate.

Acknowledgements

The authors are thankful to Dr. Anthony Gatenby at DuPont Central Research and Development, Wilmington, DE, for the plasmid directing the synthesis of molecular chaperonins GroEL and GroES.

References

1. Sugden MC, Holness MJ. Mechanisms underlying regulation of the expression and activities of the mammalian pyruvate dehydrogenase kinases. Arch Physiol Biochem 2006;112:139–149. [PubMed: 17132539]
2. Patel MS, Korotchkina LG. Regulation of the pyruvate dehydrogenase complex. Biochem Soc Trans 2006;34:217–222. [PubMed: 16545080]
3. Gudi R, Bowker-Kinley MM, Kedishvili NY, Zhao Y, Popov KM. Diversity of the pyruvate dehydrogenase kinase gene family in humans. J Biol Chem 1995;270:28989–28994. [PubMed: 7499431]
4. Rowles J, Scherer SW, Xi T, Majer M, Nickle DC, Rommens JM, Popov KM, Harris RA, Riebow NL, Xia J, Tsui LC, Bogardus C, Prochazka M. Cloning and characterization of PDK4 on 7q21.3 encoding a fourth pyruvate dehydrogenase kinase isoenzyme in human. J Biol Chem 1996;271:22376–22382. [PubMed: 8798399]
5. Kim JW, Tchernyshyov I, Semenza GL, Dang CV. HIF-1-mediated expression of pyruvate dehydrogenase kinase: a metabolic switch required for cellular adaptation to hypoxia. Cell Metab 2006;3:177–185. [PubMed: 16517405]
6. Wu P, Sato J, Zhao Y, Jaskiewicz J, Popov KM, Harris RA. Starvation and diabetes increase the amount of pyruvate dehydrogenase kinase isoenzyme 4 in rat heart. Biochem J 1998;329:197–201. [PubMed: 9405294]
7. Bowker-Kinley MM, Davis WI, Wu P, Harris RA, Popov KM. Evidence for existence of tissue-specific regulation of the mammalian pyruvate dehydrogenase complex. Biochem J 1998;329:191–196. [PubMed: 9405293]
8. Popov KM. Regulation of mammalian pyruvate dehydrogenase kinase. FEBS Lett 1997;419:197–200. [PubMed: 9428633]
9. Baker JC, Yan X, Peng T, Kasten S, Roche TE. Marked differences between two isoforms of human pyruvate dehydrogenase kinase. J Biol Chem 2000;275:15773–15781. [PubMed: 10748134]
10. Cate RL, Roche TE. A unifying mechanism for stimulation of mammalian pyruvate dehydrogenase (a) kinase by reduced nicotinamide adenine dinucleotide, dihydrolipoamide, acetyl coenzyme A, or pyruvate. J Biol Chem 1978;253:496–503. [PubMed: 201637]
11. Bao H, Kasten SA, Yan X, Hiromasa Y, Roche TE. Pyruvate dehydrogenase kinase isoform 2 activity stimulated by speeding up the rate of dissociation of ADP. Biochemistry 2004;43:13442–13451. [PubMed: 15491151]
12. Steussy CN, Popov KM, Bowker-Kinley MM Jr, Harris RA, Hamilton JA. Structure of pyruvate dehydrogenase kinase. Novel folding pattern for a serine protein kinase. J Biol Chem 2001;276:37443–37450. [PubMed: 11483605]
13. Knoechel TR, Tucker AD, Robinson CM, Phillips C, Taylor W, Bungay PJ, Kasten SA, Roche TE, Brown DG. Regulatory roles of the N-terminal domain based on crystal structures of human pyruvate dehydrogenase kinase 2 containing physiological and synthetic ligands. Biochemistry 2006;45:402–415. [PubMed: 16401071]
14. Kato M, Chuang JL, Tso SC, Wynn RM, Chuang DT. Crystal structure of pyruvate dehydrogenase kinase 3 bound to lipoyl domain 2 of human pyruvate dehydrogenase complex. EMBO J 2005;24:1763–1774. [PubMed: 15861126]
15. Hiromasa Y, Hu L, Roche TE. Ligand-induced effects on pyruvate dehydrogenase kinase isoform 2. J Biol Chem 2006;281:12568–12579. [PubMed: 16517984]

16. Tuganova A, Popov KM. Role of protein-protein interactions in the regulation of pyruvate dehydrogenase kinase activity. Biochem J 2005;387:147–53. [PubMed: 15504108]
17. Tso SC, Kato M, Chuang JL, Chuang DT. Structural determinants for cross-talk between pyruvate dehydrogenase kinase 3 and lipoyl domain 2 of the human pyruvate dehydrogenase complex. J Biol Chem 2006;281:27197–27204. [PubMed: 16849321]
18. Bao H, Kasten SA, Yan X, Roche TE. Pyruvate dehydrogenase kinase isoform 2 activity limited and further inhibited by slowing down the rate of dissociation of ADP. Biochemistry 2004;43:13432–13441. [PubMed: 15491150]
19. Kolobova E, Tuganova A, Boulatnikov I, Popov KM. Regulation of pyruvate dehydrogenase activity through phosphorylation at multiple sites. Biochem J 2001;358:69–77. [PubMed: 11485553]
20. Harris RA, Bowker-Kinley MM, Wu P, Jeng J, Popov KM. Dihydrolipoamide dehydrogenase-binding protein of the human pyruvate dehydrogenase complex. DNA-derived amino acid sequence, expression, and reconstitution of the pyruvate dehydrogenase complex. J Biol Chem 1997;272:19746–19751. [PubMed: 9242632]
21. Tuganova A, Boulatnikov I, Popov KM. Interaction between the individual isoenzymes of pyruvate dehydrogenase kinase and the inner lipoyl-bearing domain of transacetylase component of pyruvate dehydrogenase complex. Biochem J 2002;366:129–136. [PubMed: 11978179]
22. Popov KM, Kedishvili NY, Zhao Y, Gudi R, Harris RA. Molecular cloning of the p45 subunit of pyruvate dehydrogenase kinase. J Biol Chem 1994;269:29720–29724. [PubMed: 7961963]
23. Weiner MP, Costa GL, Schoettlin W, Cline J, Mathur E, Bauer JC. Site-directed mutagenesis of double-stranded DNA by the polymerase chain reaction. Gene 1994;151:119–123. [PubMed: 7828859]
24. Sanger F, Nicklen S, Coulson AR. DNA sequencing with chain-terminating inhibitors. Proc Natl Acad Sci USA 1977;74:5463–5467. [PubMed: 271968]
25. Klyuyeva A, Tuganova A, Popov KM. The carboxy-terminal tail of pyruvate dehydrogenase kinase 2 is required for the kinase activity. Biochemistry 2005;44:13573–13582. [PubMed: 16216081]
26. Laemmli UK. Cleavage of structural proteins during the assembly of the head of bacteriophage T4. Nature 1970;227:680–685. [PubMed: 5432063]
27. Lowry OH, Rosebrough NJ, Farr AL, Randall RJ. Protein measurement with the folin phenol reagent. J Biol Chem 1951;193:265–275. [PubMed: 14907713]
28. Quinn J, Diamond AG, Masters AK, Brookfield DE, Wallis NG, Yeaman SJ. Expression and lipoylation in *Escherichia coli* of the inner lipoyl domain of the E2 component of the human pyruvate dehydrogenase complex. Biochem J 1993;289:81–85. [PubMed: 8424775]
29. Korotchkina LG, Patel MS. Site specificity of four pyruvate dehydrogenase kinase isoenzymes toward the three phosphorylation sites of human pyruvate dehydrogenase. J Biol Chem 2001;276:37223–37229. [PubMed: 11486000]
30. Bowker-Kinley M, Popov KM. Evidence that pyruvate dehydrogenase kinase belongs to the ATPase/kinase superfamily. Biochem J 1999;344:47–53. [PubMed: 10548532]
31. Guex N, Peitsch MC. SWISS-MODEL and the Swiss-PdbViewer: An environment for comparative protein modeling. Electrophoresis 1997;18:2714–2723. [PubMed: 9504803]

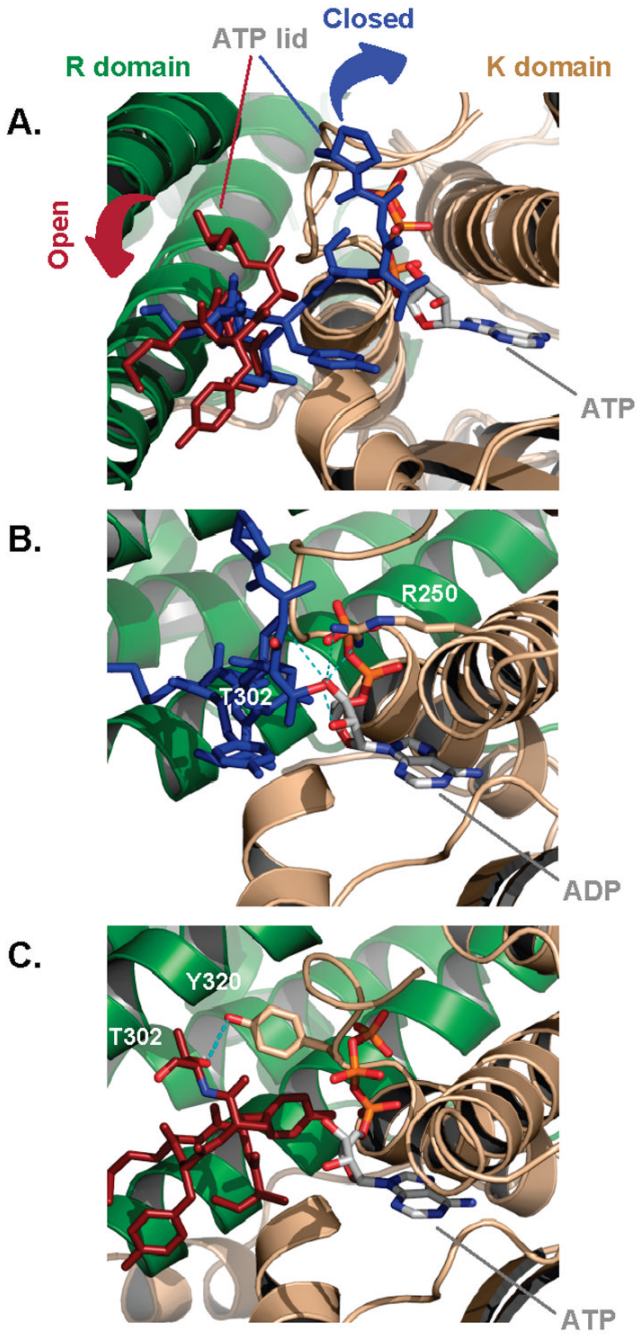

Figure 1.

"Open" and "closed" conformations of ATP lid in PDHK2 molecule. Panel A: Superimposition of the nucleotide-binding sites of PDHK2-ADP (PDB code 1jm6) (12) and PDHK2-ATP-Nov3r (PDB code 2bu2) (13) complexes. The elements of the secondary structure of R and K domains are colored in green and wheat, respectively. The amino acids of the proximal part of ATP lid (residues 296–304 in 1jm6 and 296–302 in 2bu2) are shown as stick models. The "open" conformation of ATP lid is colored in ruby red, while the "closed" conformation is colored in blue. Movement of ATP lid is indicated by blue and ruby red arrows. Bound ATP (CPK, C gray) from PDHK2-ATP-Nov3r structure is shown as stick model. The structures were superimposed using the homology-modeling program DeepView Swiss-Pdb-Viewer v3.7

(31). Panel B: The hydrogen-bonding network described by Steussy and colleagues (12) that stabilizes the “closed” conformation of ATP lid in PDHK2-ADP structure. Coloring scheme is the same as in panel A. The hydrogen bonds between T302, R250, and 2′- and 3′-hydroxyl groups of ribose are shown by dashed lines colored in cyan. Panel C: The hydrogen bond between T302 and Y320 that stabilizes the “open” conformation of ATP lid in PDHK2-ATP-Nov3r structure. The graphics were generated using the PyMOL v0.98 program (DeLano Scientific LLC, Palo Alto, CA).

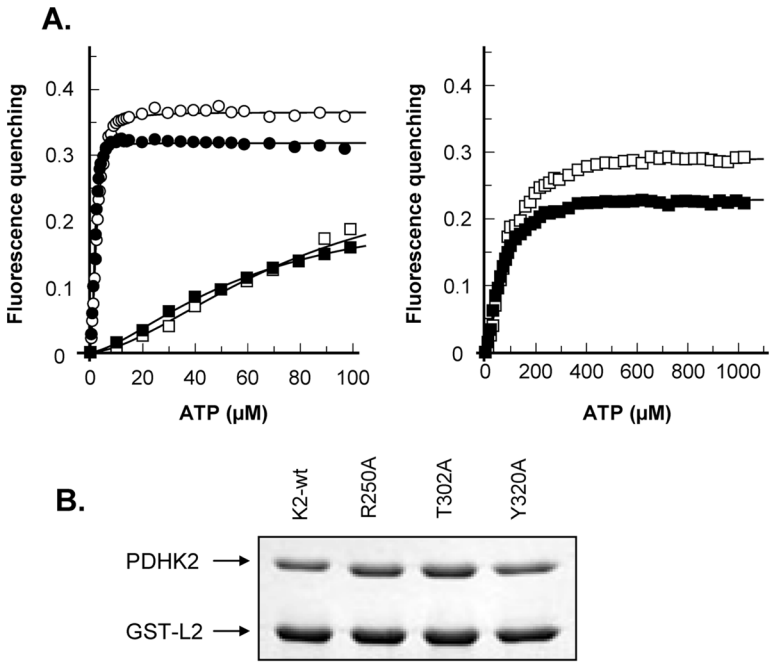

Figure 2.

Binding of nucleotide and L2 to the wild-type and mutant PDHK2 proteins. Panel A: Binding of ATP to wild-type PDHK2 (open circles), PDHK2-R250A (closed squares), PDHK2-T302A (open squares), or PDHK2-Y320F (closed circles). Measurements were made following the nucleotide-induced intrinsic fluorescence quenching of PDHK2 as described under Experimental Procedures. ATP concentration in the binding mixture was varied from 0 to 100 μM (left) or from 0 to 1000 μM (right). Panel B: Binding of the wild-type and mutant PDHK2 proteins to GST-L2. SDS/PAGE analysis of GST-L2 pull-down experiment carried out as described under Experimental Procedures. Gel was stained with Coomassie R250.

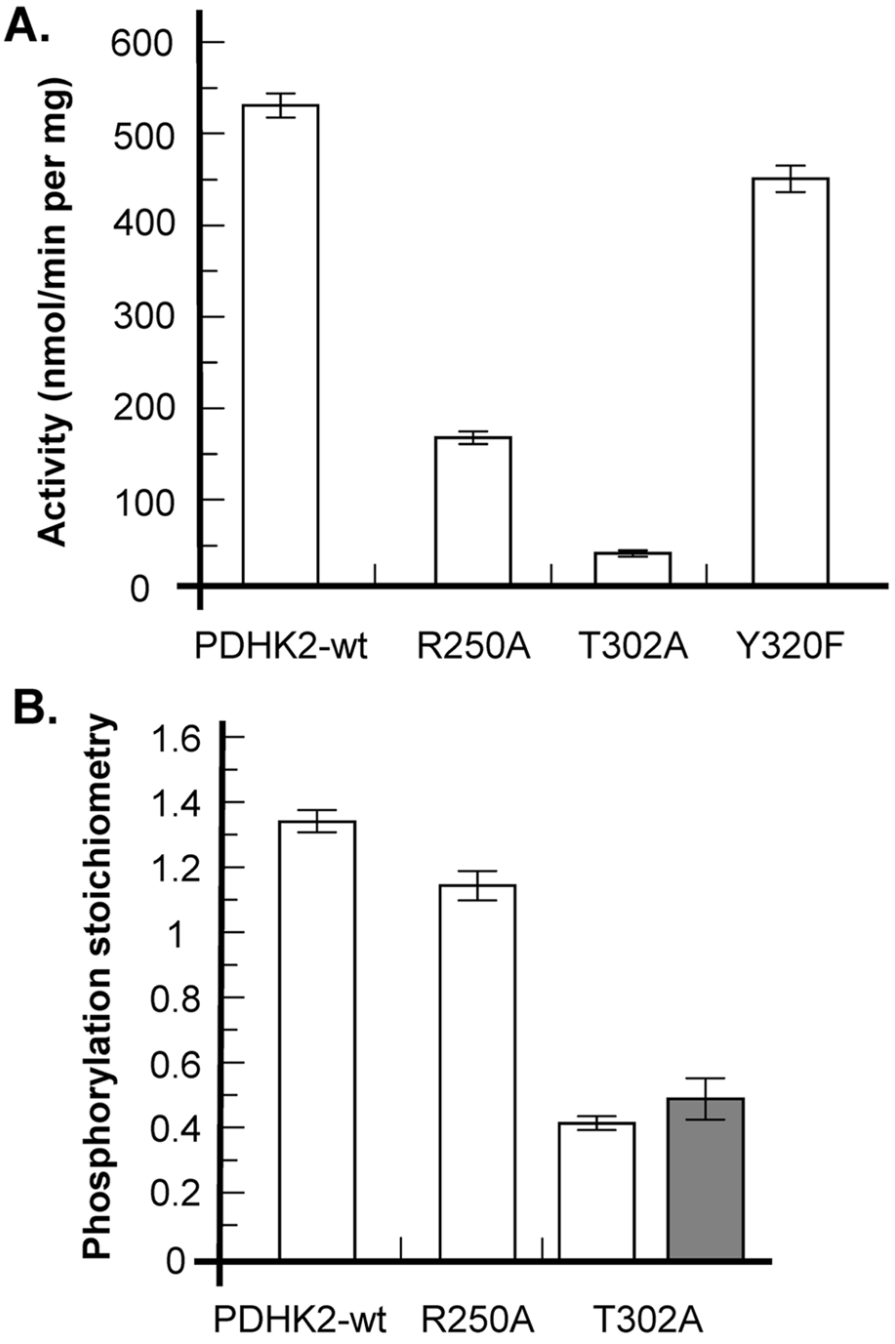

Figure 3.

Kinase activity of wild-type and mutant PDHK2 proteins. Panel A: The rates of phosphorylation of PDC by wild-type PDHK2, PDHK2-R250A, PDHK2-T302A, or PDHK2-Y320F determined under standard conditions. Panel B: Stoichiometries of PDC phosphorylation by wild-type PDHK2, PDHK2-R250A, or PDHK2-T302A. Phosphorylation reactions were carried under conditions of standard phosphorylation assay for 10 min (open bars) or 60 min (gray bar).

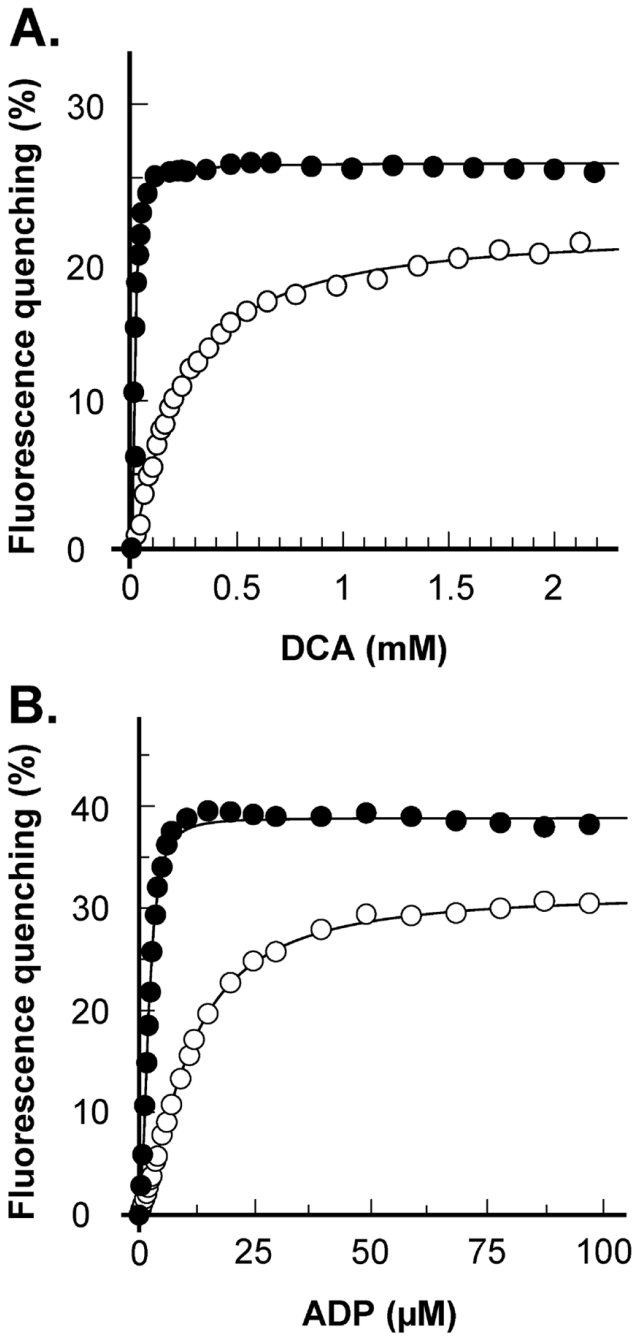

Figure 4.

Cross-talk between the nucleotide- and DCA-binding sites of PDHK2. Panel A: ADP-induced increase in DCA binding by PDHK2. Measurements were made following the DCA-induced intrinsic fluorescence quenching of PDHK2 in the absence (open circles) or in the presence (closed circles) of 50 μM ADP. DCA concentration in the binding mixture was varied from 0 to 2 mM. Panel B: DCA-induced increase in ADP binding by PDHK2 characterized using the intrinsic fluorescence quenching assay. Experiments were conducted in the absence (open circles) or in the presence (closed circles) of 0.5 mM DCA. ADP concentration in the binding mixture was varied from 0 to 100 μM.

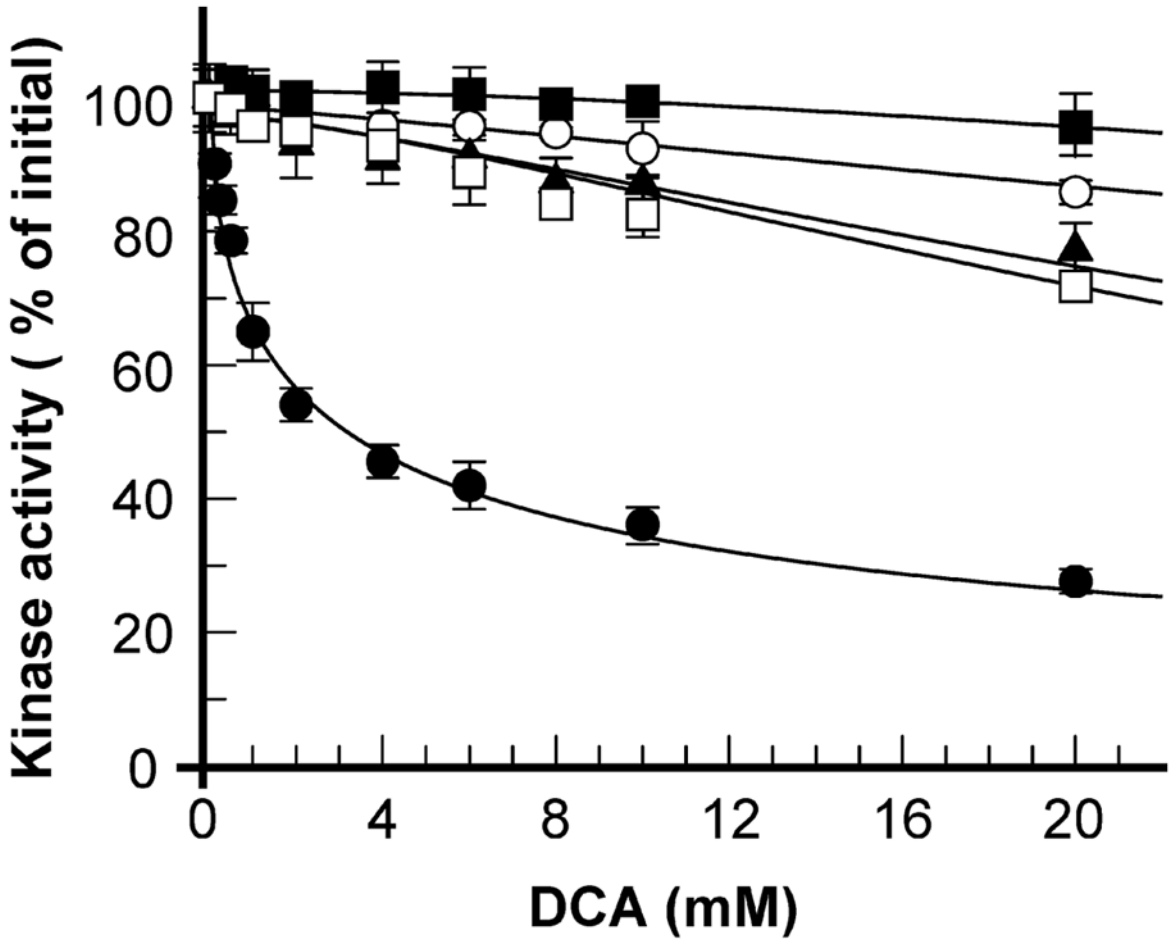

Figure 5.

Effect of DCA on kinase activity of the wild-type and mutant PDHK2 proteins. Concentration-dependent effect of DCA on kinase activity of wild-type PDHK2 (closed circles), PDHK2-R250A (closed squares), PDHK2-T302A (closed triangles), or PDHK2-Y320F (open squares). Measurements were made under the conditions of standard phosphorylation assay. Concentration-dependent effect of sodium acetate on kinase activity of wild-type PDHK2 is shown by open circles.

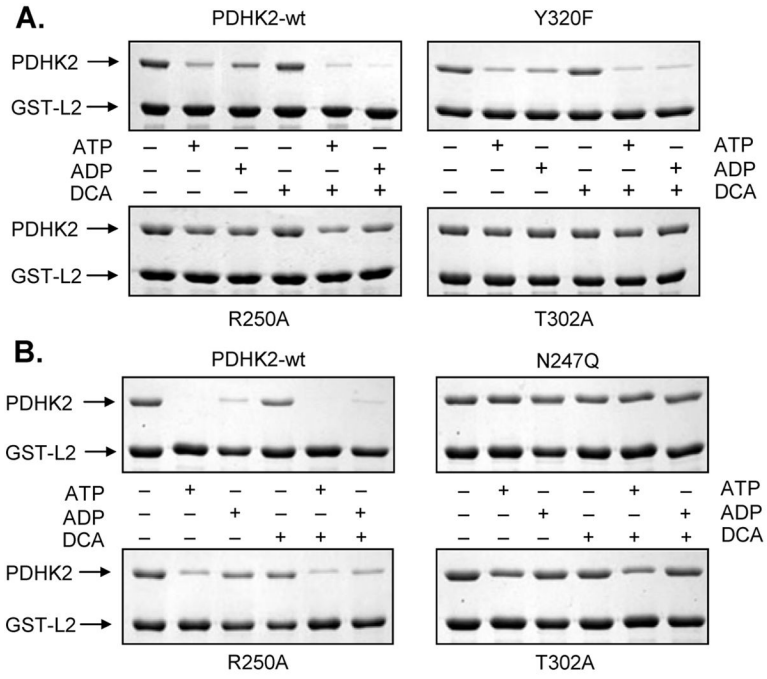

Figure 6.

Cross-talk between the nucleotide- and L2-binding sites of the wild-type and mutant PDHK2 proteins. Panel A: The effect of adenine nucleotides and DCA on the binding of wild-type and mutant PDHK2 proteins to GST-L2. SDS/PAGE analysis of GST-L2 pull-down experiment. The concentrations of adenine nucleotides and DCA in the binding mixtures were 0.5 and 1 mM, respectively. The concentration of $MgCl_2$ was 2.5 mM. Gel was stained with Coomassie R250. Panel B: SDS/PAGE analysis of GST-L2 pull-down experiment carried out with increased concentrations of adenine nucleotides (10 mM each). The concentration of $MgCl_2$ was 13 mM. Shown are the gels representative of at least three experiments.

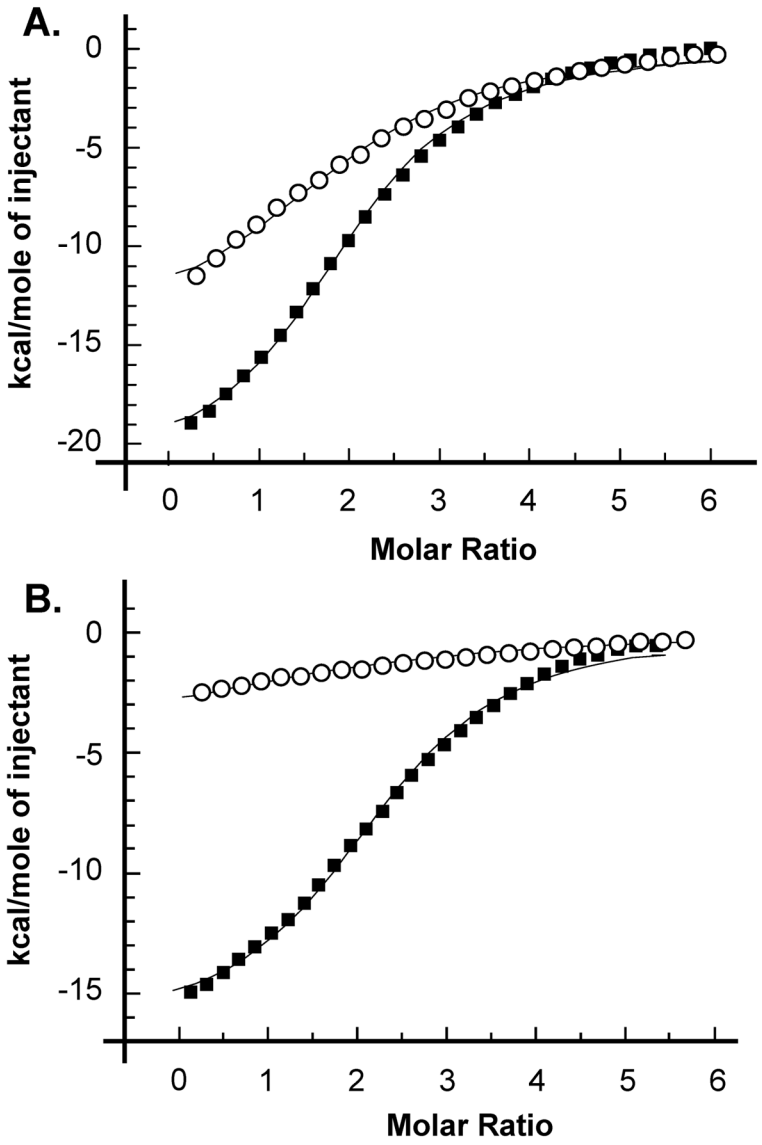

Figure 7.

Binding of L2 domain to the wild-type and mutant PDHK2. Panel A: Binding isotherms of L2 and wild-type PDHK2 (open circles) or PDHK2-T302A (closed squares). ITC measurements were performed as described under Experimental Procedures. The molar ratio represents the ratio of L2 monomer to PDHK2 dimer. Solid lines depict the least-squares fitting curves obtained using a single-site L2-binding model. Panel B: Effect of 10 mM ATP on L2 binding by wild-type PDHK2 (open circles) or PDHK2-T302A (closed squares).

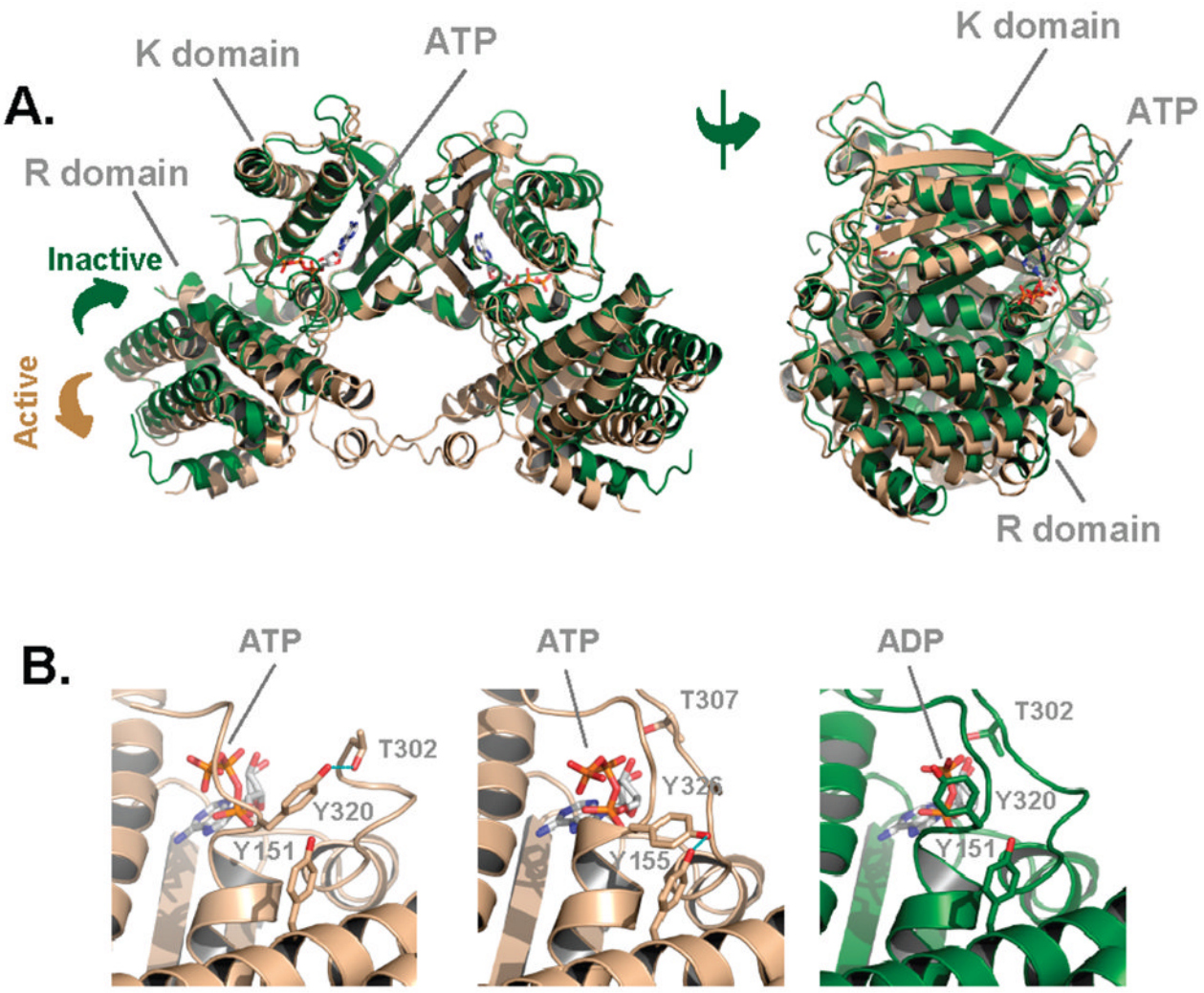

Figure 8.

"Active" and "inactive" conformations of PDHK2. Panel A: Superimposition of the dimer structure of PDHK2-ADP (green, PDB code 1jm6) onto the structure of PDHK2-ATP-Nov3r (wheat, PDB code 2bu2). Green and wheat arrows indicate the directions of interdomain hinge movement accompanied by some degree of twist. Panel B: The nucleotide-binding sites of PDHK2-ATP-Nov3r (wheat, PDB code 2bu2), PDHK3-ATP-L2 (wheat, PDB code 1y8p), and PDHK2-ADP (green, PDB code 1jm6) complexes (left, middle, and right panels, respectively). ATP, ADP, Y151 (Y155 in PDHK3), T302 (T307 in PDHK3), and Y320 (Y326 in PDHK3) are shown as stick models. The hydrogen bonds between T302 and Y320 (left panel) and between Y155 and Y326 (middle panel) are shown by dashed lines colored in cyan. The graphics were generated using the PyMOL v0.98 program.

Table 1

ATP, ADP, and DCA Binding Parameters Determined for the Wild-Type and Mutant PDHK2 Proteins

PDHK2 variants	ligand	K_d[a] (μM)	n_H[a]	Q_{max}[a] (%)
PDHK2-wt	ATP	2.5 ± 0.4	1.9 ± 0.1	37 ± 1
	ADP	10.6 ± 0.5	1.5 ± 0.2	31 ± 1
	DCA	226 ± 7	1.2 ± 0.1	21 ± 1
PDHK2-R250A	ATP	80 ± 1	1.0 ± 0.1	29 ± 1
	ADP	NM[b]		
	DCA	312 ± 25	1.0 ± 0.1	19 ± 1
PDHK2-T302A	ATP	60 ± 1	1.5 ± 0.1	23 ± 1
	ADP	NM[b]		
	DCA	320 ± 20	0.9 ± 0.1	20 ± 1
PDHK2-Y320F	ATP	1.7 ± 0.1	2.4 ± 0.1	32 ± 1
	ADP	8.9 ± 0.1	1.4 ± 0.1	24 ± 1
	DCA	292 ± 10	1.1 ± 0.1	18 ± 1

[a] ATP, ADP, and DCA binding was measured following the quenching of intrinsic tryptophan fluorescence as described under Experimental Procedures. Binding parameters were obtained by nonlinear least-squares fitting of experimental data using a cooperative ligand-binding model of the GraFit 3.09b software package (Erithacus Software Ltd., East Grinstead, West Sussex, U.K.), where K_d is the binding constant, n_H is the Hill coefficient, and Q_{max} is the extrapolated maximal quenching. Standard deviations were calculated from three to six independent determinations.

[b] NM, not measurable.

Table 2

Cross-Talk between the Nucleotide- and DCA-Binding Sites in the Wild-Type and Mutant PDHK2 Proteins

PDHK2 variants	fixed ligand	varied ligand	K_d (μM)[a]	n_H[a]	Q_{max}[a,b] (%)
PDHK2-wt	DCA (0.5 mM)	ADP	2.0 ± 0.1	2.2 ± 0.1	39 ± 1
	ADP (50 μM)	DCA	12.0 ± 0.4	1.3 ± 0.1	26 ± 1
PDHK2-R250A	DCA (0.5 mM)	ADP	NM[c]		
	ADP (50 μM)	DCA	161 ± 4	1.2 ± 0.1	38 ± 1
	ADP (500 μM)	DCA	59 ± 1	1.9 ± 0.1	45 ± 1
PDHK2-T302A	DCA (0.5 mM)	ADP	NM[c]		
	ADP (50 μM)	DCA	249 ± 9	1.1 ± 0.1	23 ± 1
	ADP (500 μM)	DCA	103 ± 1	1.3 ± 0.1	38 ± 1
PDHK2-Y320F	DCA (0.5 mM)	ADP	2.5 ± 0.2	1.9 ± 0.1	37 ± 1
	ADP (50 μM)	DCA	33 ± 1	1.2 ± 0.1	29 ± 1

[a] Binding experiments were conducted essentially as described in the legend to Table 1. Standard deviations were calculated from three to six independent determinations.

[b] Q_{max} represents fluorescence quenching caused by the varied ligand (fluorescence quenching caused by the fixed ligand was treated as 0% quenching and was not included in Q_{max}).

[c] NM, not measurable.